Eur. Phys. J. A **17**, 317–321 (2003)
DOI 10.1140/epja/i2002-10173-x

THE EUROPEAN PHYSICAL JOURNAL A

Proton elastic form factor: The JLab data

C.F. Perdrisat[1,a] and the Jefferson Lab Hall A Collaboration[2]

[1] College of William and Mary, Williamsburg, VA 23187, USA
[2] Thomas Jefferson National Accelerator Facility, Newport News, VA 23606, USA

Received: 1 November 2002 /
Published online: 15 July 2003 – © Società Italiana di Fisica / Springer-Verlag 2003

Abstract. The ratio of the electric and magnetic proton form factors, G_{Ep}/G_{Mp}, has been obtained in two Hall A experiments, from measurements of the longitudinal and transverse polarization of the recoil proton, P_L and P_T, respectively, in the elastic scattering of polarized electrons, $\mathbf{e}p \rightarrow e\mathbf{p}$. Together these experiments cover the Q^2 range 0.5 to 5.6 GeV^2. A new experiment is currently being prepared, to extend the Q^2 range to 9 GeV^2 in Hall C.

PACS. 13.40.Gp Specific reactions and phenomenology: Electromagnetic form factors – 14.20.Dh Properties of specific particles: Protons and neutrons – 24.70.+s Nuclear reactions: Polarization phenomena in reactions

1 Introduction

The nucleon elastic form factors describe the internal structure of the nucleon; in the non-relativistic limit, for small four-momentum transfer squared, Q^2, they are Fourier transforms of the charge and magnetization distributions in the nucleon. At high Q^2 values, the nucleon must be treated as a system of three valence quarks; perturbative QCD predicts the Q^2-dependence [1] of the form factors. At Q^2 between 1 and 10 GeV^2, relativistic constituent quark models [2,3] currently give the best understanding of the nucleon form factors, with the strongest dynamical input; Vector Meson Dominance (VMD) (see, *e.g.*, refs. [4,5]) also describes the form factors well.

The unpolarized elastic ep cross-section is given by

$$\frac{\mathrm{d}\sigma}{\mathrm{d}\Omega} = \frac{\alpha^2 E_e^{'} \cos^2\frac{\theta_e}{2}}{4E_e^3 \sin^4\frac{\theta_e}{2}} \left[G_{Ep}^2 + \frac{\tau}{\epsilon} G_{Mp}^2\right] \left(\frac{1}{1+\tau}\right), \qquad (1)$$

where G_{Ep} and G_{Mp} are the electric and magnetic form factors, $\epsilon = [1 + 2(1+\tau)\tan^2(\frac{\theta_e}{2})]^{-1}$, θ_e is the scattering angle of the electron in the laboratory and $\tau = Q^2/4M_p^2$, with M_p the proton mass; E_e and $E_e^{'}$ are the energies of the in- and outgoing electrons, respectively. For a given Q^2, G_{Ep} and G_{Mp} can be extracted from cross-section measurements made at fixed Q^2, over a range of ϵ values with the Rosenbluth method. At Q^2 below 1 GeV^2, G_{Ep} and G_{Mp} have been determined by this method and $\mu_p G_{Ep}/G_{Mp}$ has been found to be ≈ 1. At larger Q^2, the cross-section becomes dominated by the G_{Mp} contribution; G_{Mp} is known up to $Q^2 = 31$ GeV^2 [6]. In fig. 1, the error bars on $\mu_p G_{Ep}/G_{Mp}$ from the World cross-section data (refs. [7–13]) are seen to grow with Q^2. Above $Q^2 \approx 1$ GeV^2, systematic differences between different experiments are evident.

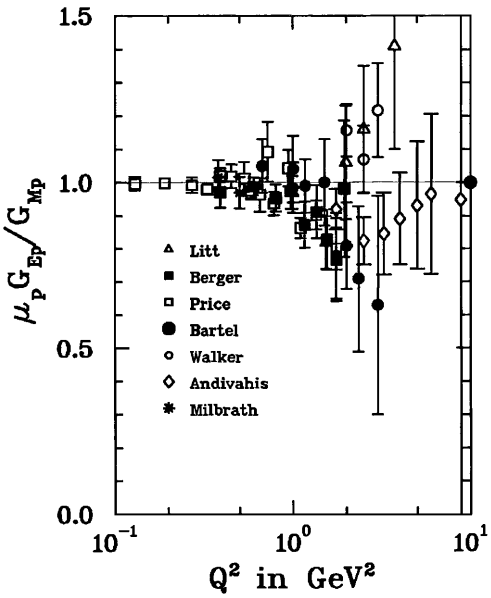

Fig. 1. World data for $\mu_p G_{Ep}/G_{Mp}$ *versus* Q^2 , not including the JLab polarization data.

The JLab results have been obtained by measuring the recoil proton polarization in $\mathbf{e}p \rightarrow e\mathbf{p}$ [14,15]. In one-photon exchange, the scattering of longitudinally polarized electrons on unpolarized hydrogen results in a

[a] e-mail: perdrisa@jlab.org

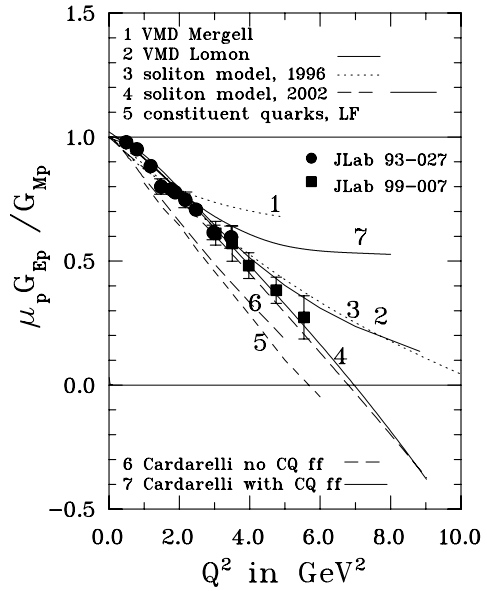

Fig. 2. Comparison between $\mu_p G_{Ep}/G_{Mp}$ measured at JLab and several theoretical models; the JLab data are from refs. [14] and [15].

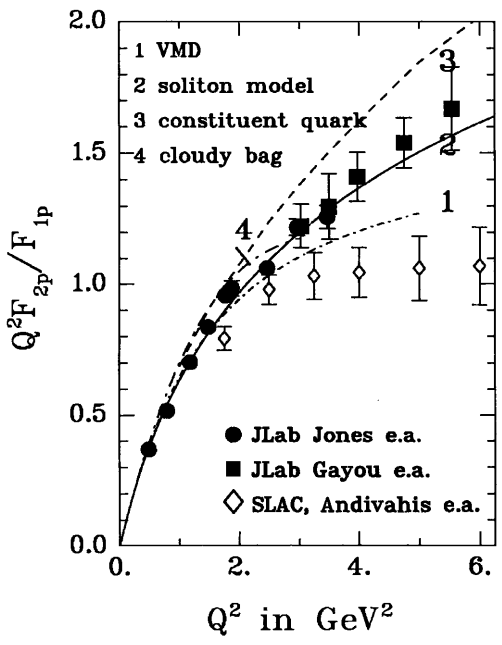

Fig. 3. The ratio Q^2F_{2p}/F_{1p} from the JLab experiments, compared with the data of ref. [12].

transfer of polarization to the recoil proton with two components, P_T perpendicular to, and P_L parallel to the proton momentum in the scattering plane [16]:

$$I_0 P_T = -2\sqrt{\tau\,(1+\tau)} G_{E_p} G_{M_p} \tan\frac{\theta_e}{2}\,, \qquad (2)$$

$$I_0 P_L = \frac{1}{M_p}\,(E_e + E_{e'})\,\sqrt{\tau\,(1+\tau)} G_{M_p}^2 \tan^2\frac{\theta_e}{2}\,, \qquad (3)$$

where $I_0 \propto G_{E_p}^2 + \frac{\tau}{\epsilon} G_{M_p}^2$. Measuring simultaneously these two components and taking their ratio gives the ratio of the form factors:

$$\frac{G_{Ep}}{G_{Mp}} = -\frac{P_T}{P_L}\frac{(E_e + E_{e'})}{2M_p}\tan\left(\frac{\theta_e}{2}\right). \qquad (4)$$

Neither the beam polarization nor the analyzing power of the polarimeter, used to measure P_T and P_L, appear in eq. (4).

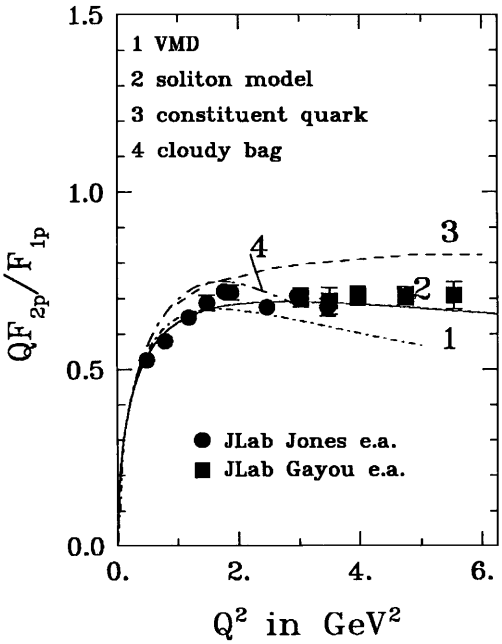

Fig. 4. The ratio QF_{2p}/F_{1p} discussed in the text.

2 Experiments

In 1998 G_{Ep}/G_{Mp} was measured for Q^2 from 0.5 to 3.5 GeV^2 [14]. Protons and electrons were detected in coincidence in the two high-resolution spectrometers (HRS) of Hall A. The polarization of the recoiling proton was measured in a graphite analyzer focal-plane polarimeter (FPP). In 2000 new measurements were made at $Q^2 = 4.0$, 4.8 and 5.6 GeV^2 with overlap points at $Q^2 = 3.0$ and 3.5 GeV^2 [15]. To extend the measurement to these higher Q^2, two changes were made. First, to increase the figure-of-merit of the FPP, a CH_2 analyzer was used; the thickness was increased from 50 cm of graphite to 100 cm of CH_2 (60 cm for $Q^2 = 3.5$ GeV^2). Second, the electrons were detected in a lead-glass calorimeter with 9 columns and 17 rows of $15 \times 15 \times 35$ cm^3 blocks placed so as to achieve complete solid-angle matching with the HRS detecting the proton. At the largest Q^2 the solid angle of the calorimeter was 6 times that of the HRS.

The combined results from both experiments are plotted in fig. 2 as the ratio $\mu_p G_{Ep}/G_{Mp}$. If the $\mu_p G_{Ep}/G_{Mp}$-ratio continues its linear decrease with the same slope, it will cross zero at $Q^2 \approx 7.5$ GeV^2. In fig. 2, calculations based on VMD [4], a relativistic constituent quark (CQ) [2], and a soliton model [17] are shown. Also shown

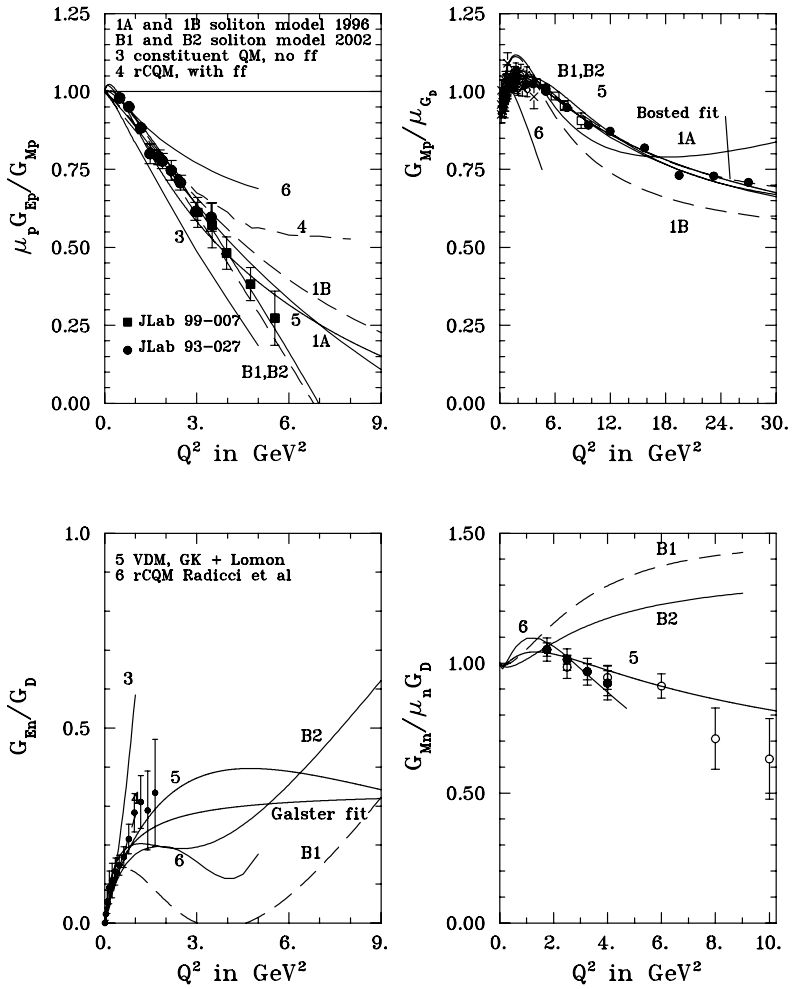

Fig. 5. Theoretical predictions for G_E and G_M of the proton and neutron, along with selected data. For G_{En} only the results of a recent analysis of elastic ed data from ref. [18] are shown; for G_{Mn} only the larger Q^2 data of refs. [19] and [20] are shown. Curves labeled "Bosted fit" and "Galster fit" are from refs. [21] and [22], respectively.

are results with another relativistic CQ model (rCQM) [3], with and without CQ form factor. Lomon [5] has reworked the Gary-Krumpelman VMD model [23] and obtained good agreement with the data for reasonable parameters for the vector-meson masses and coupling constants.

3 Results and discussion

In fig. 3 the JLab data are shown as Q^2 times F_2/F_1; pQCD predicts quenching of the spin flip form factor F_2, or equivalently helicity conservation; higher-order contributions should make Q^2F_2/F_1 asymptotically constant. The data clearly contradict this prediction.

Shown in fig. 4 is Q times F_2/F_1, which reaches a constant value at $Q^2 \sim 2$ GeV^2. Ralston *et al.* [24] have proposed that this scaling is due to the non-zero orbital-angular-momentum part of the proton quark wave function. Miller and Frank [25] have shown that imposing Poincarè invariance leads to violation of the helicity conservation rule, and reproduces the QF_2/F_1 behavior.

More demanding for models are predictions for all four form factors of the nucleon. The VMD fits are done in terms of the isoscalar and isovector form factors and thus naturally include all four form factors. In fig. 5 predictions from the rCQM with $SU(6)$ symmetry breaking [3], the soliton model [17], the point form model [26], and the VMD model of ref. [5] are shown. The soliton model does well only for the proton. The recent VMD analysis [5] reproduces G_{Ep}, G_{Mp} and G_{Mn} well, and predicts larger values for G_{En} than the fit of ref. [22], in agreement with the preliminary data of ref. [27].

Isospin invariance at the quark level requires that F_2/F_1 become the same for proton and neutron starting at some large Q^2 value. In fig. 6 we show the prediction for QF_2/F_1 and Q^2F_2/F_1 for proton and neutron from ref. [5]; F_2/F_1 may become equal for the proton and the neutron for $Q^2 > 10$ GeV^2. The evolution of QF_2/F_1 at small Q^2 is dominated by the charge neutrality of the neutron, which results in $F_{1n} = 0$ at $Q^2 = 0$. A future experiment in JLab Hall A [28], to measure G_{En} up to 3.4 GeV^2, will significantly improve our knowledge of the nucleon form factors.

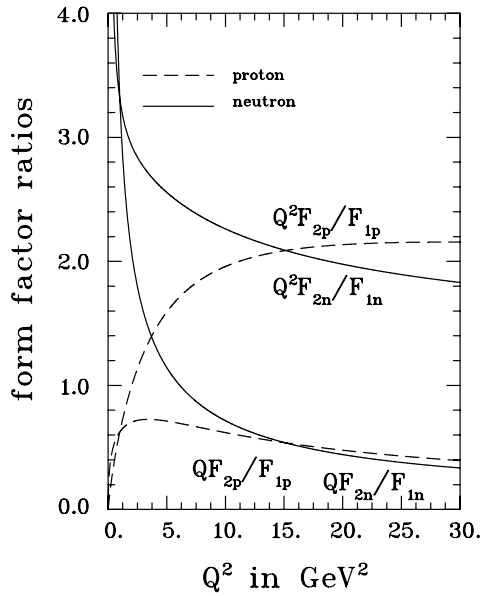

Fig. 6. The ratios QF_2/F_1 and Q^2F_2/F_1 for proton and neutron, from ref. [5]: both ratios tend toward the same value for proton and neutron above 15 GeV^2; neither one of these ratios becomes constant below this same Q^2, a marked difference to the proton ratio.

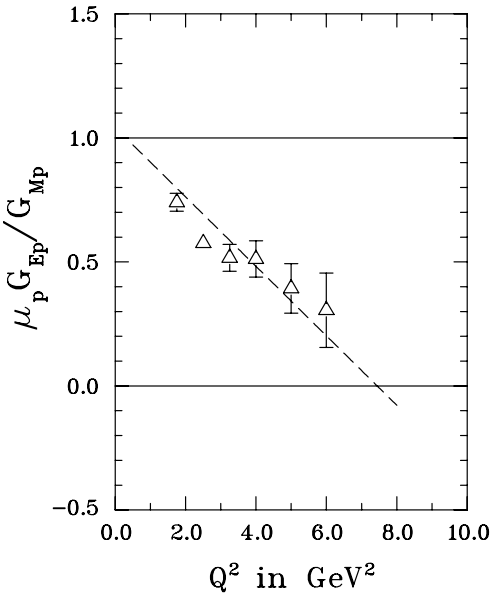

Fig. 7. Ratios $\mu_p G_{Ep}/G_{Mp}$ recalculated from the data of ref. [12] but without the renormalisation factor used in this publication. The dashed line is the best linear fit to the JLab data.

Answering the anticipated question, whether the new JLab polarization data could be reconciled with the older cross-section data shown in fig. 1, we point out the following facts. First, the 1971 and 1973 data of refs. [8,10], although with large uncertainties, are entirely compatible with the new data; in fact their authors, at the time, claimed to have observed a clear deviation from 1 for the $\mu_p G_{Ep}/G_{Mp}$-ratio which we have now observed with much better accuracy. Second, the latest cross-section data of Andivahis required a renormalisation of the smallest ϵ data point, which was measured in the SLAC 1.6 GeV spectrometer, to the cross-sections obtained with the 8 GeV spectrometer used for all other ϵ values. The factor was 0.958 ± 0.007 obtained for the lowest Q^2 point, and applied to the lowest ϵ data point at all Q^2's. We show in fig. 7, which is based on the unrenormalised cross-sections published in [12], that if this renormalisation is removed, the corresponding Rosenbluth $\mu_p G_{Ep}/G_{Mp}$-ratios are entirely compatible with the JLab polarization data.

4 Conclusion

The precise new JLab data on $\mu_p G_{Ep}/G_{Mp}$ show that this ratio continues to drop off linearly with increasing Q^2 up to 5.6 GeV^2. The ratio F_2/F_1 does not follow the $1/Q^2$ behavior predicted by pQCD; this is a distinct signature of the non-perturbative regime dominating the Q^2 range of the two JLab experiments described here. This behavior must be compared with the scaling of $Q^4 G_{Mp}$ seen in ref. [6], which has been interpreted as indicative of pQCD for the magnetic form factor of the proton. Comparison of model calculations to the JLab data provides a stringent test of models of the nucleon.

I thank my colleagues V. Punjabi, M. Jones, E. Brash, L. Pentchev and O. Gayou for their essential roles in the completion of these experiments. The Southeastern Universities Research Association manages the Thomas Jefferson National Accelerator Facility under DOE contract DE-AC05-84ER40150. U.S. National Science Foundation grant PHY 99 01182 supports my research.

References

1. S.J. Brodsky, G.P. Lepage, Phys. Rev. D **22**, (1981) 2157.
2. M.R. Frank, B.K. Jennings, G.A. Miller, Phys. Rev. C **54**, 920 (1996).
3. E. Pace, G. Salme, F. Cardarelli, S. Simula, Nucl. Phys. A **666** & **667**, 33c (2000); F. Cardarelli, S. Simula, Phys. Rev. C **62**, 65201 (2000).
4. P. Mergell, U.G. Meissner, D. Drechsler, Nucl. Phys. A **596**, 367 (1996) ; A.W. Hammer, U.G. Meissner, D. Drechsel, Phys. Lett. B **385**, 343 (1996).
5. E. Lomon, Phys. Rev. C **64**, 035204 (2001) and nucl-th/0203081.
6. A.F. Sill *et al.*, Phys. Rev. D **48**, 29 (1993).
7. J. Litt *et al.*, Phys. Lett. B **31**, 40 (1970).
8. Ch. Berger *et al.*, Phys. Lett. B **35**, 87 (1971).
9. L.E. Price *et al.*, Phys. Rev. D **4**, 45 (1971).
10. W. Bartel *et al.*, Nucl. Phys. B **58**, 429 (1973).
11. R.C. Walker *et al.*, Phys. Rev. **49**, 5671 (1994).
12. L. Andivahis *et al.*, Phys. Rev. D **50**, 5491 (1994).
13. B. Milbrath *et al.*, Phys. Rev. Lett. **80**, 452 (1998); **82**, 221 (1999) (E).
14. M.K. Jones *et al.*, Phys. Rev. Lett. **84**, 1398 (2000).
15. O. Gayou *et al.*, Phys. Rev. Lett. **88**, 092301 (2002)

16. A.I. Akhiezer, M.P. Rekalo, Sov. J. Part. Nucl. **3**, 277 (1974); R. Arnold, C. Carlson, F. Gross, Phys. Rev. C **23**, 363 (1981).
17. G. Holzwarth, Z. Phys. A **356**, 339 (1996).
18. R. Schiavilla, I. Sick, Phys. Rev. C **64**, 041002 (2001), nucl-ex/0107004.
19. A. Lung *et al.*, Phys. Rev. Lett. **70**, 718 (1993).
20. S. Rock *et al.*, Phys. Rev. Lett. **49**, 1139 (1982).
21. P.E. Bosted, Phys. Rev. **51**, 409 (1995).
22. S. Galster *et al.*, Nucl. Phys. B **32**, 221 (1971).
23. M.F. Gari, W. Krumpelmann, Phys. Lett. B **274**, 159 (1992).
24. J. Ralston *et al.*, in *Proceedings of the 7th International Conference on Intersection of Particle and Nuclear Physics, Quebec City (2000)*, edited by Z. Parseh, W. Marciano (AIP, New York, 2000) p. 302, and private communication (2001).
25. G.A. Miller, M.R. Frank, Phys. Rev. C **65**, 065205 (2002), nucl-th/0201021.
26. R.F. Wagenbrunn, S. Boffi, W.H. Klink, W. Plessas, M. Radici, Phys. Lett. B, **511**, 33 (2001).
27. See R. Madey *et al.*, this issue, p. 323.
28. G. Cates, K. McCormick, B. Reitz, B. Wojtsekhowski *et al.*, JLab approved proposal 02-013 (2002).